CHAPTER 87

TWO-DIMENSIONAL EMPIRICAL EIGENFUNCTION MODEL FOR THE ANALYSIS AND PREDICTION OF BEACH PROFILE CHANGES

T.-W. Hsu¹, S.-R. Liaw², S.-K. Wang² and S.-H. Ou³

ABSTRACT

A two-dimensional empirical eigenfunction model is proposed for the analysis and the prediction of beach profile change due to longshore and cross-shore sediment transports. Beach profile data from Redhill coast, Taiwan, measured every two months at 150 meters interval along the detached breakwaters are analyzed and the relative importance from two directions is investigated. Furthermore, by employing the method of Markov process and linear regression, a prediction model is formulated which takes into account the effect of breaking waves, bottom sediment and radiation stress of waves. This 2-D model is shown to be effective in the analysis and the prediction of beach changes near the coastal structures.

INTRODUCTION

The movement of coastal sediment can be decomposed into longshore component and cross-shore component. Longshore transport is defined as sediment transport parallel to the beach, while cross-shore transport is defined as transport perpendicular to the beach. These components are both significant in response to seasonal variations in the forcing parameters such as waves, tides, winds and currents. Therefore, beach profile changes due to longshore and crossshore transport should be separated and represented as a time series in order to obtain a detailed understanding.

Winant et al.(1975) proposed a method to describe beach changes in terms of empirical eigenfunctions. The usefulness of the eigenfunctional representation was confirmed as а concise method of representing beach profile changes

1180

Graduate student, MS. Eng. MS. Eng., former graduate student Dr. Eng., Professor and Chairman

³

Department of Hydraulics and Ocean Engineering National Cheng Kung University, Tainan, Taiwan 70101 Republic of China

(Aubrey, 1978; Aranuvachapun and Johnson, 1979). Uda and Hashimoto (1982) proposed a new model to analyze the beach changes due to longshore and cross-shore sediment transports. They used longshore eigenfunctions and cross-shore eigenfunctions to describe temporal variations of beach profile changes. However, the cross-shore eigenfunctions were taken as a time average in their analysis and only the longshore eigenfunctions changing with time. This implies that the beach profile change is independent of cross-shore sediment transport.

The aim of this paper is to extend Uda and Hashimoto's concept and proposes a 2-D empirical eigenfunction model for the analysis and the prediction of beach profile changes for temporal and spatial variation where both longshore and cross-shore sediment transport are significant. Field observation of beach profiles obtained from Redhill, Taiwan, are examined and the relative importance of beach changes from two orthogonal modes is also given. In addition, a prediction model is formulated by employing the method of Markov process and linear regression. The results of prediction model are compared with the existing models and measured data.

THEORETICAL FORMULATION

One-Dimensional Empirical Eigenfunction Method

The method has been described by Winant et al. (1975). In brief, an eigenfunction is expressed in the form of

$$h_{xt} = \sum_{n} e_{nx} C_{nt}$$
(1)

where the $h_{x,t}$ are the beach profile data, $e_{n,x}$ represent the spatial eigenfunctions, $C_{n,t}^{*}$ represent temporal eigenfunctions, and n represent the variation modes.

The spatial eigenfunctions form an orthogonal set as

$$\sum_{n=1}^{\infty} e_{nx} e_{mx} = \delta_{nm} \tag{2}$$

where δ_{nm} is Kronecker delta.

The spatial correlation matrix A is expressed as

$$A = \begin{bmatrix} a_{11} & a_{12} & a_{13} & . & . & a_{1n} \\ a_{21} & a_{22} & a_{23} & . & . & a_{2n} \\ . & . & . & . & . \\ . & . & a_{1j} & . \\ . & . & . & . \\ a_{n1} & a_{n2} & a_{nj} & . & . & a_{nn} \end{bmatrix}$$
(3)

In which, the elements of matrix A are defined by

$$a_{ij} = \frac{1}{N_x N_t} \sum_{i} h_{it} h_{jt} \qquad (4)$$

where N_x is the number of data points per profile, N_t is the

number of measured times. The matrix A possesses a set of eigenvalues λ_n and a set of corresponding eigenfunctions $e_{n\,x}$ which are defined by matrix equation

$$A e_{nx} = \lambda_n e_{nx}$$
 (5)

The temporal eigenfunctions are calculated with

$$C_{nt} = \sum_{x} h_{xt} e_{nx}$$
(6)

By defining $C_{nt}=C_{nt}/(\lambda_n N_x N_t)^{1/2}$, it can be shown that C_{nt} form an orthogonal set, and eq.(1) is rewritten as

$$h_{xt} = \sum_{n} (\lambda_n N_x N_t)^{1/2} e_{nx} C_{nt}$$
(7)

Analysis of 2-D Empirical Eigenfunction Method

Following Uda and Hashimoto (1982), we extend the 1-D empirical eigenfunction method to the 2-D bed elevation h(x,y,t), which is a function of offshore distance x, and longshore distance y at a certain time t. The expression of h(x,y,t) is as follow

$$h(x,y,t) = \sum e_k(x,t) e_k(y,t)$$
(8)

In this expression, $e_k(x,t)$ are the cross-shore eigenfunc-tions, $e_k(y,t)$ the longshore eigenfunctions, k the variation modes. Eq.(8), obviously, represents the variation of the beach profile configuration in terms of longshore and cross-shore distances at the specific time t. In some cases, such as the profile configuration around a coastal structure or a rhythmic topography, it is desirable to use the data of all changes instead of the single beach profile. The cross-shore eigenfunctions form an orthogonal set

as

$$\sum_{\mathbf{x}} \mathbf{e}_{\mathbf{n}}(\mathbf{x}, \mathbf{t}) = \delta_{\mathbf{n}\mathbf{m}}$$
(9)

In order to generate the cross-shore eigenfunctions, like the correlation matrix A, a symmetric matrix B is formed with elements of

$$b_{ij} = \frac{1}{N_x N_y} \sum_{y} h(i,y,t) h(j,y,t)$$
(10)

where Ny denotes the total number of measured points alongshore. The matrix B are real matrix with a set of eigenvalues λ_k and a set of corresponding eigenfunctions $e_k(x,t)$

$$Be_k(x,t) = \lambda_k e_k(x,t) \tag{11}$$

The longshore eigenfunctions $e_k(y,t)$ which define the longshore changes of beach profile are evaluated as

$$e_{k}(y,t) = \sum_{x} h(x,y,t) e_{k}(x,t)$$
(12)

In the analysis of beach profile changes due to longshore and cross-shore sediment transports, Uda and Hashimoto (1982) took the cross-shore eigenfunctions $e_k(x,t)$ to be independent of time and only let the longshore eigenfunctions $e_k(x,t)$ to be fin-dependent of time and only let the longshore eigenfunctions $e_k(y,t)$ changing with time. This means that the nature of variations doesn't depend on cross-shore sediment transport. This paper allows $e_k(x,t)$ and $e_k(y,t)$ to vary with distance and time respectively. The expressions of $e_k(x,t)$ and $e_k(y,t)$ are given as follows,

$$e_k(x,t) = \sum_n (\lambda_n N_x N_t)^{1/2} e_k^n(x) C_{kx}^n(t)$$
 (13)

$$e_k(y,t) = \sum_{n} (\lambda_n N_x N_t)^{1/2} e_k(y) C_{ky}(t)$$
 (14)

where $e_k^n(x)$: cross-shore spatial eigenfunctions $C_{kx}^{n}(t)$: cross-shore temporal eigenfunctions $e_k^{\mathbf{m}}(\mathbf{y})$: longshore spatial eigenfunctions $C_{ky}^{m}(t)$: longshore temporal eigenfunctions

Formulation of the Prediction Model

In order to relieve forecast errors, the variation of beach profile subtracted the mean beach profile from the original data is used. By this method, the set h(x,y,t) is expressed as

$$h(x,y,t) = \overline{h}(x,y) + \sum_{k} e_{k}(x,t) e_{k}(y,t)$$
(15)

where $\overline{h}(x,y)$ is the temporal mean of the beach profile. A prime on the eigenfunctions indicates that these eigenfunctions are similar in data sets where the mean profile has not been removed. According to eqs.(13) and (14), $e_k'(x,t)$ and $e_k'(y,t)$ can be expressed, respectively, in the form of 1

$$e_{k}'(x,t) = \sum_{n} (\lambda_{nx} N_{x} N_{t})^{1/2} e_{k}^{n}(x) C_{kx}^{n}(t)$$
 (16)

1

.

$$e_{k}'(y,t) = \sum_{k} (\lambda_{my} N_{x} N_{t})^{1/2} e_{k}^{m'}(y) C_{ky}^{m'}(t)$$
 (17)

The fluctuations of beach profile are calculated as

$$h'(x,y,t) = h(x,y,t) - h(x,y)$$
 (18)

h'(x,y,t) was used to generate eqs.(16) and (17) by processing the procedure of the analysis of 2-D empirical eigenfunction method.

The predictands for prediction model always consist of a representation of the beach profile time series. Accordingly, it is necessary to forecast the next time step eigenfunctions $C_n(i+1)$ and let the spatial eigenfunctions $e_k(x)$ and $e_k(y)$ to be constants. The Markov process based on Sonu (1973) and three forcing parameters were used here to estimate the temporal eigenfunctions $C'_{n(i+1)}$ in the prediction model. The simplest linear equations can be described as

$$\begin{bmatrix} C'_{1 (i+1)} &= \overline{a_{11}}C'_{1i} + \overline{a_{12}}C'_{2i} + \dots + \overline{a_{1n}}C'_{ni} + \overline{a_{1(n+1)}}F_{i+1} \\ C'_{2 (i+1)} &= \overline{a_{21}}C'_{1i} + \overline{a_{22}}C'_{2i} + \dots + \overline{a_{2n}}C'_{ni} + \overline{a_{2(n+1)}}F_{i+1} \\ \vdots \\ C'_{n (i+1)} &= \overline{a_{n1}}C'_{1i} + \overline{a_{n2}}C'_{2i} + \dots + \overline{a_{nn}}C'_{ni} + \overline{a_{n(n+1)}}F_{i+1} \\ (19) \\ \begin{bmatrix} C'_{1 (i+1)} \\ C'_{2 (i+1)} \\ \vdots \\ C'_{n (i+1)} \end{bmatrix} = \begin{bmatrix} \overline{a_{11}} & \overline{a_{12}} & \dots & \overline{a_{1n}} & \overline{a_{1(n+1)}} \\ \overline{a_{21}} & \overline{a_{22}} & \dots & \overline{a_{2n}} & \overline{a_{2(n+1)}} \\ \vdots & \vdots & \vdots \\ \overline{a_{n1}} & \overline{a_{n2}} & \dots & \overline{a_{nn}} & \overline{a_{n(n+1)}} \end{bmatrix} \begin{bmatrix} C'_{1i} \\ C'_{2i} \\ \vdots \\ F_{i+1} \end{bmatrix}$$
(20)

where $\overline{a_{1\,i}}$... $\overline{a_{n\,(n+1)}}$ are constant coefficients, F_{i+1} are the dimensionless forcing parameters for the next time step.

Three forcing parameters corresponding to breaking waves, features of bottom sediment transport and radiation stresses of waves were taken into account in the present method. The reason why these three parameters are chosen is that they have been used in the past with degrees of success to describe nearshore process. Based on Battjes (1974), the characteristics of breaking waves can be described by surf similarity parameter ζ defined by

$$\zeta = \tan \beta / (H/L_0)^{1/2}$$
(21)

where $\tan\beta$ is the bottom slope, H wave height, L₀ wave length in deep water. The features of bottom sediment transport can be classified by the parameter C proposed by Gourlay (1968)

$$C = H_0 / WT$$
(22)

where w is the fall velocity of sediment determined by the characteristics of sand and kinematic viscosity of the fluid and T is the wave period. The radiation stresses of inclined waves are written as (Bowen, 1969)

$$S = \begin{bmatrix} S_{XX} & S_{XY} \\ S_{YX} & S_{YY} \end{bmatrix} = \begin{bmatrix} S_{TT} \cos^2 \alpha + S_{SS} \sin^2 \alpha & (S_{TT} - S_{SS}) \sin \alpha & \cos \alpha \\ (S_{SS} - S_{TT}) & \sin \alpha & \cos \alpha & S_{TT} \sin^2 \alpha + S_{SS} \cos^2 \alpha \\ (23) \end{bmatrix}$$

with

$$S_{rr} = E(2n-1/2)$$
, $S_{ss} = E(n-1/2)$, $E = 1/8 \rho g H^2$

where r is the direction of wave propagation, s is the direction normal to the wave propagation, x is cross-shore coordinate, y is longshore coordinate, α is the angle be-

or

tween wave crest and beach, n is the ratio of wave group velocity to wave celerity, E is wave energy, ρ is density and g is gravity acceleration. A dimensionless wave energy was introduced for the consistent dimension of forcing parameters

$$\mathbf{E}_{0} = (1/8 \ \rho \, \mathrm{gH}^{2}) \ / \ (1/8 \ \rho \, \mathrm{gH}^{2}) \tag{24}$$

It is convenient to write eq.(19) in general matrix notation as

$$\mathbf{P} = \overline{\mathbf{A}} \cdot \mathbf{D} \tag{25}$$

where P is the $(\mathbf{m} \cdot \mathbf{N})$ matrix of m quantities to be predicted, D is the $(\mathbf{n} \cdot \mathbf{N})$ matrix of n data parameters and $\overline{\mathbf{A}}$ is an $(\mathbf{m} \cdot \mathbf{n})$ coefficient matrix, N is the total number of observations of these quantities which are to be used in the prediction. The optimal form of the coefficient matrix $\overline{\mathbf{A}}$ was determined by using the linear regression:

$$A = C_{PD} C_{DD}^{-1} = (P \cdot D^{T}) (D \cdot D^{T})^{-1}$$
(26)

where C_{PD} denotes the covariance matrix between the predictand and data, C_{DD} is the auto-covariance matrix of the data, and T is the transpose operator.

The estimator of matrix P is used for both hindcast and forecast models. A hindcast model is defined as the estimate made from the same data and the predictand which are used to form the covariance matrix, whenas a forecast model is defined as the estimate made from the covariances formed from other data and predictand samples. According to Davis (1976), the hindcast skill can be represented by a predictability index $S_{\rm H}$:

. .

$$S_{H} = 1 - \frac{E(P-\bar{P}) (P-\bar{P})^{T}}{E(PP^{T})}$$
(27)

in which E represents the expected value operator, \hat{P} denotes the estimated value. The hindcast skill increases with the higher value of S_H. On the other hand, the forecast ability was described by the mean-square-forecast error S_F:

$$S_{F} = \frac{E[h(x,y,t) - h(x,y,t)][h(x,y,t) - h(x,y,t)]^{T}}{E[h(x,y,t)][h(x,y,t)]^{T}}$$
(28)

where h(x,y,t) is the estimated bed elevation. A model is predictable with lower mean-square-forecast error.

FIELD DATA

Beach Profile Data

As shown in Fig.1, Redhill coast is located in the southern part of Taiwan and consists of eroding sandy bluffs ranging from 6 to 10 meters high. Fig.2 shows the detached breakwaters built on the shoreline to prevent waves from reaching the eroding shore.

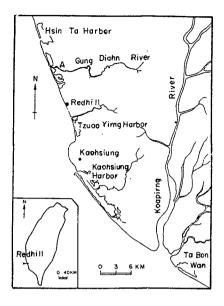


Fig. 1 Location of Redhill coast

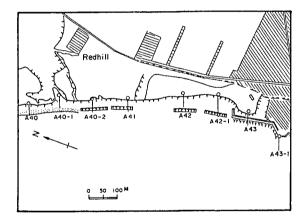


Fig. 2 Alignment of detached breakwaters and observed positions

The beach sand has median grain size of 0.28mm and submerged specific gravity of 1.6 Surveys of the beach profile have been conducted at every two months from 1982 to 1984. Each profile was measured at some intervals over a distance about 600m offshore. A detailed measurement was done on the foreshore part by using standard surveying method, while depth measurements on the offshore part were taken by cable lead.

Wave Climate of Redhill Coast

There are no wave data available at Redhill coast. The wave data observed at Ta Bon Wan located about 48km south of Redhill coast (Fig.1) have been used. The wave height at Ta Bon Wan was measured at the depth of 12.5 meters using a pressure wave gage. In winter, the prevailing direction of incoming wave at Ta Bon Wan is NNE, and waves from various directions were partly sheltered by land. The cumulative relative energy $P_E(\theta)$ is given by

$$P_{E}(\theta) = \frac{1}{m_{0}} \int_{-\pi/2}^{0} \int_{0}^{\infty} S(f,\theta) df d\theta \qquad (29)$$

where $S(f,\theta)$ is directional wave spectrum, f is angular frequency, θ is the azimuth measured counterclockwise, and mo is the total wave energy expressed as

$$m_{0} = \int_{-\pi/2}^{\pi/2} \int_{0}^{\infty} S(f,\theta) df d\theta$$
 (30)

For NNE directional waves, the azimuths θ_1 and θ_2 were taken as -45° and 31° for Redhill coast and for Ta Bon Wan, respectively. The wave height ratio k_d between Redhill coast and Ta Bon Wan is determined by using SWOP directional spectrum

$$k_d = \sqrt{P_E(\theta_1) / P_E(\theta_2)} = 3.15 \tag{31}$$

In summer, since the SW directional incoming wave is almost perpendicular to the coast, wave data from Ta Bon Wan can be directly applied to Redhill coast without any modification.

Based on Sawaragi (1982), the response of the beach to the various kinds of incident waves can be expressed in terms of a representative wave calculated by the following formulas:

representative wave period: $T_s = \sum_i T_i p_i / P_T$ (32)

representative wave height: $H_{s}^{2}C_{gs}P_{T} = \Sigma C_{gi}H_{i}^{2}p_{i}$ (33)

representative wave direction: $H_s^2C_{gs} \sin \alpha_s \cos \alpha_s P_T = \Sigma H_1^2C_{g1} \sin \alpha_1 \cos \alpha_1 p_1$ (34)

where H_i: component wave height

H_s: representative wave height

Ti: component wave period

T_s: representative wave period α_i : component wave direction α_s : representative wave direction C_{gi}: representative wave group velocity p_i: component probability P_T = $\sum_{i=1}^{n} p_i = total$ probability

RESULTS AND DISCUSSION

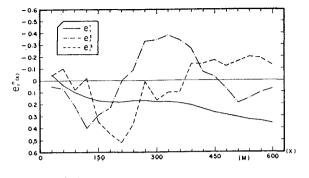
Results of Beach Profile Analysis

The 2-D empirical eigenfunction analysis was conducted by using the beach profile data collected at Redhill coast from December, 1982 to December, 1984. The total number of recording times is $N_t=13$ and that of calculating points $N_x=20$, $N_y=8$.

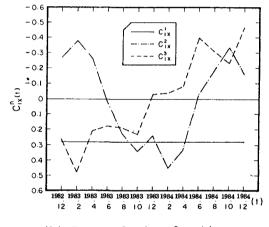
Fig.3(a) shows the cross-shore profiles of section A40-2 of the first three spatial eigenfunctions e_1^1 (solid line), e_1^2 (dash-dot line) and e_1^3 (dash line). The temporal eigenfunctions are given by $C_{1x}^{1}(solid line)$, $C_{1x}^{2}(dash-dot line)$ and C_{1x}^{3} (dash line) as shown in Fig.3(b). The first spatial eigenfunction is interpreted as the mean beach function according to Winant et al. (1975). The time dependence of the mean beach function is almost constant, indicating a stable beach for Redhill coast. The second spatial eigenfunction has a minimum at the location of summer berm and a maximum in the area of winter bar. The negative value of the second temporal eigenfunction accounts for the sand migration up to the level of the summer berm, while the positive value indicates the movement of sand down beach to the winter bar and hence represents erosion on the beach. The third spatial eigenfunction has positive value in the broad region from shoreline to about 400m and negative value in the offshore region. The corresponding temporal eigenfunction is found to have positive values before December, 1983 and negative values after December, 1983.

The 2-D empirical eigenfunction method is also employed for the analysis of shoreline changes due to the construction of detached breakwaters. Based on Uda and Hashimoto (1982), the shoreline changes can be described in terms of the second longshore eigenfunctions $e_2(y,t)$. From Fig.4, we note that the second longshore eigenfunction changes with seaward advancement at the central side on which the detached breakwaters were constructed. The corresponding cross-shore eigenfunction $e_2(x,t)$ is shown in Fig.5, in which the cross-section of a detached breakwater is located about 30m in the x direction. Depositions of sand behind the detached breakwater is also found. Results of analysis reveal that the design and the construction measures.

Fig.6(a) presents the first three longshore spatial eigenfunctions e_1^1 (solid line), e_1^2 (dash-dot line) and e_1^3 (dash line). The time variations of these functions as shown in Fig.6(b) are C_{1y}^1 (solid line), C_{2y}^2 (dash-dot line)



(a) Spatial eigenfunction



(b) Temporal eigenfunction

Fig. 3 The first three crossshore eigenfunctions (section A40-2)

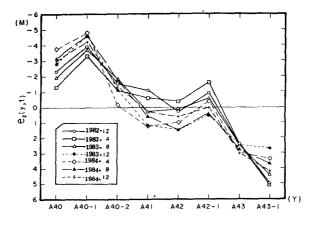


Fig. 4 The second longshore eigenfunctions e2(y,t)

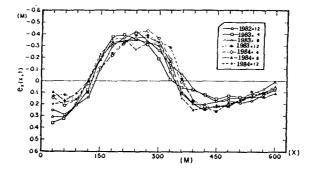
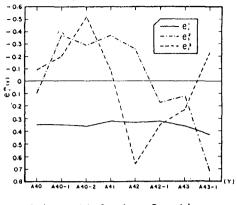


Fig. 5 The second cross-shore eigenfunctions $e_2(x,t)$



(a) Spatial eigenfunctions

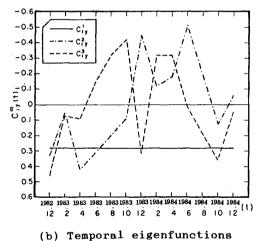


Fig. 6 The first three longshore eigenfunctions

and C_{1y}^3 (dash line). The temporal function C_{1y}^1 shows almost no chang over the recording time. The other two eigenfunctions show no clear tendency. Perhaps more data are required for the analysis.

On the other hand, Winant et al. (1975) pointed out that each eigenvalue is representative of certain percentage of the mean square value of the data. Table 1 shows that the eigenvalues of longshore eigenfunctions are larger that those of cross-shore eigenfunctions, indicating that the longshore sediment transport has more effect on beach profile change than the cross-shore sediment transport does.

Prediction of Beach Profile Changes

It has been shown that the stability is an important consideration in the prediction of empirical eigenfunction method (Aubrey, 1978). In this paper, two data sets of different sample lengths (N_t=10 and 12) were examined. The results of analysis show that the eigenfunctions are stable with respect to the length of the data (Wang, 1985).

Uda and Hashimoto (1982) calculated the shoreline change by one-line theory, and then the longshore eigenfunction $e_2(y,t)$ was calculated from shoreline changes. Since the nearshore zone is characterized by complex flow fields and fluid-sediment interactions, it is difficult to estimate quantitative shoreline changes by one-line simulation. The correlation between $e_2(y,t)$ and shoreline changes is not significant in present analysis as shown in Fig.7. In this paper, three parameters and computed beach configuration at each time step are used to predict temporal eigenfunctions, because they are easily to obtain from available wave data and beach profile data without any mathematical simulation.

Table 2 shows the mean square value of forecast error S_F for different models. The forecast skill of present analysis is better than 1-D model and Uda and Hashimoto's model, although its predictability S_E was lower as listed in Table 3.

Fig.8(a) and (b) depict two profiles of A40-2 and A41 and their estimates from three different models. It is seen that the prediction of 2-D model yields a better result than 1-D model and Uda and Hashimoto's model as compare to the measured profiles.

component	longshore eigenfunctions			cross-shore eigenfunctions		
mode		=	Ξ	-	.=	Ξ
1	0.124871	0.093681	0.092341	0.049939	0.038738	0.038335
2	0.000050	0.029298	0.029826	0.000029	0.009608	0.009192
3	0.000034	0.000861	0.001430	0.000022	0.001074	0.001438
4	0.000024	0.000702	0.000705	0.000005	0.000191	0.000453
5	0.000011	0.000277	0.000510	0.000002	0.000138	0.000168

Table 1 A comparison of eigenvalues between longshore and cross-shore eigenfunctions

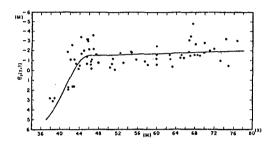


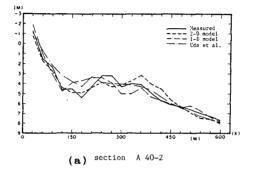
Fig. 7 A relationship between longshore eigenfunction $e_2(\mathbf{y},t)$ and shoreline changes

Table 2 Mean square error Sr for three different models

Sec. No.	I — D	2 - D	Hashimoto and Uda	
A 40	0.0193	0.0083	0.0215	
A 40 - 1	0.0194	0. 020 0	0.0294	
A 40 - 2	0.0151	0.0137	0.0147	
A 41	0.0107	0.0071	0.0137	
A 42	0.0224	0.0153	0.0233	
A 42 - 1	0.0262	0.0093	0.1122	
A 43	0.0107	0.0105	0.0215	
A 43 - 1	0.0068	0.0142	0.0291	

Table 3 Predictability index S_H for 1-D and 2-D model

I → D	Sec. No.	Sн	Sec. No.	S _H	
	A 40	0.8282	A 42	0.8545	
	A 40 - 1	0.8409 A 42-1		0.8550	
	A 40 - 2	0.8669	A 43	0.8130	
	A 41	0.9021	A 43-1	0.8005	
2-D	cross-shore	0.7857	iongshore	0.6089	



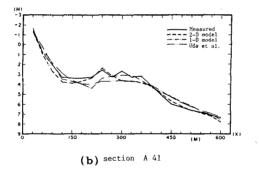


Fig. 8 Comparison of predicted results

CONCLUSION

Field data of beach profiles taken over two years at coast were analyzed by employing the 2-D empirical Redhill The results indicate that beach eigenfunction method. due to longshore and cross-shore sediment profile changes transports are separable. A successful detached breakwater as beach erosion countermeasure is also verified. The pre-diction of 2-D model shows that the beach profile changes The preare predictable. It is also concluded that this 2-D model is shown to be effective in the analysis and the prediction of beach changes near coastal structures.

REFERENCES

- Aranuvachapun, S. and J.A. Johnson: Beach profiles at Gorleston and Great Yarmouth, Coastal Eng., (1)pp.201-203, 1979.
- Aubrey, D.G.: Statistical and dynamical prediction of (2) changes in natural sand beaches, Ph.D. dissertation, Univ. of Calif., San Diego, 194pp. 1978. Battjes, J.A.: Surf similarity, Proc. 14th ICCE, ASCE,
- (3)pp.466-480, 1974.
- Bowen, A.J.: The generation of longshore currents on a plane beach, J. Fluid Mech., pp.206-215, 1969. Davis, R.E.: Predictability of sea surface temperature (4)
- (5) and sea level pressure anomalies over the North Pacific Ocean, J. Phys. Oceanogr., vol.6, no.3, pp.249-266,1976. Gourlay, M.S.,: Beach and dune erosion tests, Delft
- (6)
- Hydraulics Laboratory, Report no. M935/M936, 1968. Sawaragi, T.: Sediment and beach erosion, Morikata (7) Publication Company, Japan, 195pp., 1982. Sonu, C.J.: A Markov model for beach change,
- (8) J.
- Geophys. Res., vol.78, no.9, pp.1462-1471, 1973. Uda, T. and H. Hashimoto: Description of beach changes (9)using an empirical predictive model of beach profile
- (10) Wang, S.K.: On the analysis and the prediction of the two-dimensional beach topographical changes, M.S. thesis, National Cheng Kung Univ., Tainan, Taiwan, 51pp., 1985.
- (11) Winant, C.D., D.L. Inman and C.E. Nordstrom: Description of seasonal beach changes using empirical eigenfunctions, J. Geophys. Res., vol.8, no.15, pp.1979-1986, 1975.